Particle decay from the giant resonance region of ^{40}Ca †

D. H. Youngblood, A. D. Bacher,* D. R. Brown, J. D. Bronson,
J. M. Moss, and C. M. Rozsa

Cyclotron Institute and Physics Department, Texas A & M University, College Station, Texas 77843
(Received 12 July 1976)

The reactions ^{40}Ca$(\alpha, 2\alpha)^{36}$Ar and ^{40}Ca$(\alpha, \alpha p)^{39}$K have been studied at 115-MeV bombarding energy in order to obtain the charged particle decay characteristics of the giant quadrupole resonance at $E_x = 18.0$ MeV. Energy and angle were measured for both outgoing light particles to completely define the kinematics. Weak proton decay to the $d_{3/2}$ ($\Gamma_{p_0}/\Gamma = 0.08^{+0.05}_{-0.03}$) and $s_{1/2}$ ($\Gamma_{p_1}/\Gamma = 0.22^{+0.05}_{-0.08}$) hole states of ^{39}K was observed from the giant quadrupole resonance while most of the decay proceeded to the region of the $d_{5/2}$ hole states. While the $(\alpha, 2\alpha)$ reaction populated the ^{36}Ar ground state (0^+), 1.97-MeV state (2^+), and 4.18–4.44-MeV states (4^+, 3^-), only upper limits could be established for α decay of the giant quadrupole resonance ($\Gamma_{\alpha_0}/\Gamma < 0.06$). Significant decay of the 14-MeV $L = 2$ state to the ground state of ^{36}Ar was observed ($\Gamma_{\alpha_0}/\Gamma \sim 0.9 \pm 0.2$).

> NUCLEAR REACTIONS ^{40}Ca$(\alpha, \alpha p)$, $(\alpha, 2\alpha)$, $E_\alpha = 115$ MeV; measured $d^4\sigma/d\Omega_\alpha d\Omega_p dE_\alpha dE_p$, $d^4\sigma/d\Omega_\alpha d\Omega_\alpha dE_\alpha dE_\alpha$, α-p angular correlation giant quadrupole resonance decay; deduced branching ratios, giant quadrupole resonance.

INTRODUCTION

There has been considerable recent interest in giant multipole resonances in addition to the well-known giant dipole resonance (GDR). Studies with inelastic electron[1] and hadron[2, 3] scattering on many nuclei have revealed a broad state lying in the vicinity of the GDR. The excitation energy of this peak is approximately $63/A^{1/3}$ MeV, in agreement with theoretical estimates for the location of the isoscalar $E2$ giant resonance. Inelastic electron scattering angular distributions of this peak are characteristic of an $L = 2$ or $L = 0$ state (for even-even nuclei), while angular distributions for inelastic proton,[2] deuteron,[4] ^{3}He,[5] and α^3 scattering are in general fitted either better by $L = 2$ or equally well by $L = 0$ distorted wave born approximation (DWBA) calculations. For several reactions[3] the strength in this peak would far exceed the sum rule if the state were monopole. The strong excitation of this peak by α particles[3] confirms the isoscalar nature of the phenomena. Thus the preponderance of the evidence suggests that this is the isoscalar giant quadrupole resonance (GQR).

Recently Meyer-Schützmeister et al.[6] have observed with the ^{54}Fe (α, γ) ^{58}Ni reaction a peaking of $E2$ strength consistent with the inelastic scattering results; however, other attempts to locate this strength with proton and α capture reactions (primarily for sd shell and lighter nuclei) have not been successful. A detailed comparison of available radiative capture data with α scattering for light nuclei[7] reveals no actual discrepancy between the two types of measurements. For $A \lesssim 32$ the $E2$

strength as determined from inelastic scattering is broadly spread out, in agreement with radiative capture measurements. In ^{40}Ca, where a narrow concentration of $E2$ strength ($\sim 42\%$ of the energy weighted sum rule in a peak of width ~ 3.5 MeV) is seen by inelastic scattering,[3] careful mapping of the $E2$ strength has not been accomplished with capture reactions. A study of the ^{36}Ar(α, γ) ^{40}Ca reaction by Branford[8] revealed no peaking of $E2$ strength in the expected region although he concludes that his data are not inconsistent with the existence of a giant quadrupole resonance of $E_x \sim 18$ MeV. The ^{39}K(p, γ) ^{40}Ca (Ref. 9) and ^{40}Ca(γ, p) (Ref. 10) reactions are dominated by the GDR, which gives a peak of 3.1 MeV width located at $E_x = 19.3$ MeV, completely overshadowing the GQR. The ratio of $E2$ to $E1$ strength can be estimated using the appropriate sum rules[11]:

Isovector $E1$:

$$\sigma_0^{E1} = \int o \, dE = \frac{2\pi^2 e^2 \hbar}{mc} \frac{NZ}{A} = \frac{60 NZ}{A} \text{ MeV mb};$$

Isoscalar $E2$:

$$\sigma_{-2}^{E2} = \int \frac{o}{E^2} \, dE = \frac{\pi^2}{137} \frac{Z^2}{3A} \frac{\langle r^2 \rangle}{mc^2} = 0.4 \frac{Z^2}{A^{1/3}} \text{ MeV}^{-1} \mu b.$$

For ^{40}Ca these give $\sigma_0^{E1} = 600$ MeV mb and $\sigma_{-2}^{E2} = 47$ MeV^{-1} μb. Assuming the GDR exhausts $\sim 55\%$ of the $E1$ sum rule and has a Lorentzian distribution, it is estimated that at the peak of the GQR the $E2/E1$ ratio is 0.033 in strength or 18% in amplitude. If the fractional decay to the ground state of ^{39}K is comparable for these two resonances, the $E2$ strength could be seen through its interference

with the $E1$ in the angular distribution of capture
γ radiation. However, within experimental un-
certainties, no evidence for peaking of $E2$ strength
was seen for ^{40}Ca excitation energies from 18.1
to 21 MeV in the (p, γ) experiment. Proton and α
decay thresholds are about 7–8 MeV in ^{40}Ca so that
there are many states in ^{39}K and ^{36}Ar to which
decay of the GQR is energetically allowed. Neutron
decay to the ground state of ^{39}Ca is also possible,
and decay to ^{39}Ca excited states is possible for the
upper part of the GQR. Although $2p$ and 2α decay
channels are energetically allowed, they should be
severely hindered by the Coulomb barrier.

It was partially to help clarify this disagreement
between inelastic scattering and (p, γ) experiments
that prompted the present investigation. As the
GQR is prominent in inelastic α scattering[3, 7] on
^{40}Ca and excitation of the GDR is isospin forbidden,
the decay of the GQR was studied by detecting pro-
tons and α particles in coincidence with α particles
inelastically scattered from ^{40}Ca. Proton decay
branches to simple hole states in ^{39}K are a mea-
sure of the one-particle–one-hole components of
the GQR.

EXPERIMENTAL PROCEDURE

The 115-MeV α particle beam from the Texas
A & M University cyclotron, after energy analysis,
bombarded self-supporting natural Ca foils located
in the Ortec 76.2-cm scattering chamber. The
beam was stopped and the charge collected in a
Faraday cup located 2 m behind the chamber. One
to three ΔE-E-veto silicon detector telescopes
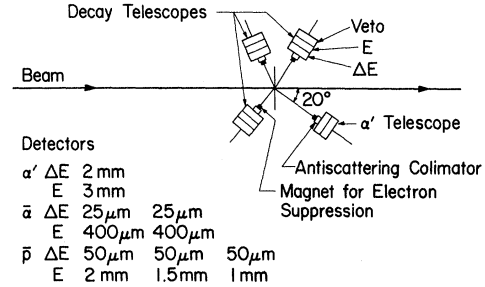

FIG. 1. A schematic diagram of the experimental
geometry. The decay telescopes were mounted on a
single turntable which rotated relative to the α' detector.

were used simultaneously to detect protons (2–15
MeV) or α particles (5–26 MeV) while one ΔE-E
telescope fixed at 20° detected high energy α
particles (75–115 MeV). The experimental geom-
etry is illustrated in Fig. 1. Conventional elec-
tronics were used for particle identification with
each stack as well as for fast timing between the
α' stack and the decay stacks. A block diagram of
the electronics is shown in Fig. 2. To reduce
pileup in the relatively slow particle identifiers,
linear gates after the amplifiers permitted pas-
sage of pulses only when a fast coincidence be-
tween the α' stack and one of the decay stacks
occurred. Single-channel analyzers were used to
select appropriate particle groups for each de-
tector stack. The energy signals were then rou-
ted into two analog to digital converters and thence
to a PDP-15 computer, along with tag information
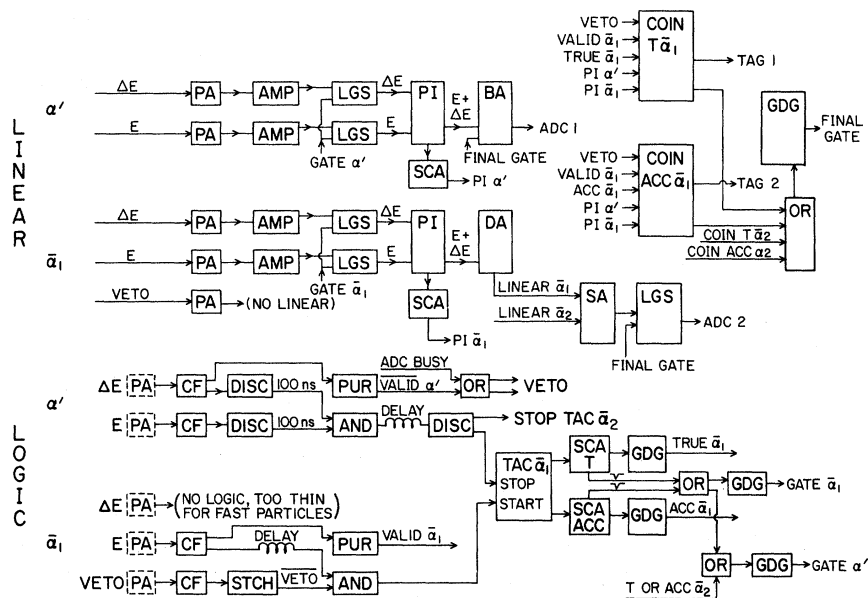to identify the decay stack and to classify the

FIG. 2. A block diagram of the electronics. Only one decay stack is indicated.

event as a true or accidental coincidence. The data were stored event by event on tape for later analysis. Six 64-×64-channel two-dimensional arrays corresponding to true and accidental coincidences between events in each decay stack and events in the α' detector were stored live. In addition 12 512-channel spectra corresponding to projections on each axis of the above spectra were stored for continuous monitoring of the progress of the experiment. Pulser signals were also recorded in the computer (identified by a unique tag) for all stacks during data acquisition to provide a continuous monitor of the proper operation of all circuits. Timing and particle identifier windows were monitored in multichannel analyzers.

Counting rates were maintained at ~50 kHz for the α' stack while rates in the decay stacks varied from 5–35 kHz. Pileup rejection was accomplished by rejecting all events for which two fast timing signals in the same stack arrived within a time window of 3 μsec; 20–35% of the events were rejected on this basis. The large angular openings (~5° in each stack) and the high rates resulted in an energy resolution of approximately 500 keV in all of the stacks. The time resolution was about 10 nsec, comparable to the beam pulse width.

The beam was focused to a ~1-mm wide by ~3-mm high spot in the center of the target. The beam axis was located to within 0.3° by rotating each detector stack into the "beam" resulting from the few ions produced in the cyclotron with no ion source arc current. A 2.5-mm thick Ta shield prevented beam "halo" from striking the target frame. Checks were performed to ensure that background contributions from nontarget sources were negligible in the manner described previously.[3] The self-supporting natural Ca targets, 2.5 cm square and 1–3 mg/cm² thick, were prepared by vacuum evaporation. As the $^{16}O(\alpha, 2\alpha)$ and $^{16}O(\alpha, \alpha p)$ reactions can contribute in the re-

gions of interest, care was taken to minimize the oxygen contaminant in the Ca foils. The targets, after evaporation, were mounted on target frames and transferred to the scattering chamber in an argon atmosphere resulting in an $^{16}O/^{40}Ca$ atomic ratio of $\lesssim 0.04$.

Special care was taken to obtain proton and α decay probabilities. The target thicknesses were determined with an ^{241}Am α source using the energy loss technique. Singles data were taken during coincidence runs by deleting appropriate coincidence requirements. Decay branches observed in the coincidence measurements were then related to the singles measurements by accounting for the different integrated current and the solid angle of the detector for the decay particle. The target thickness and solid angle of the α' detector remained the same.

EXPERIMENTAL RESULTS AND DATA ANALYSIS

Data were taken in a series of experimental runs as listed in Table I. The α' detector was fixed at 20° for all the runs, resulting in a recoil angle of approximately -65° for $^{40}Ca^*$ excited in the 20-MeV region. The angles for the detectors of the decay particles were chosen for approximately even coverage from 0° to 180° in the recoil system. One run was undertaken to check the relative p and α decay by remeasuring the data at the same angle pairs used in the previous runs. As only relative normalization was being checked, these runs were fairly short with insufficient statistics to observe details of the decay.

A spectrum of inelastic α particles obtained at 20° with the coincidence geometry is shown in Fig. 3. There are several groups for which p or α decay might be observed. Around $E_x \sim 12$ MeV there is a group of states which, taken as a whole ($\Gamma \sim 1$ MeV), have a nondescript (α, α') angular

TABLE I. Experimental runs for $^{40}Ca^*$ decay. The detector angles and accumulated charge (Q) are given for each run.

Run	Reaction	$\theta_{\alpha'}$	θ_p [a]	$\theta_{\bar{\alpha}}$ [a]	Q (μC)
1	$\bar{\alpha}, p$	20°	-122° ($\phi = 30°$)	+67°	1790
2	p	20°	-65°, -125°, +145°		2304
	p	20°	-90°, -150°, +120°		1289
3	$\bar{\alpha}$	20°		-60°, -120°	1587
	$\bar{\alpha}$	20°		-82°, -142°	1726
4	$\bar{\alpha}$	20°		-60°	992
	$\bar{\alpha}$	20°		+120°	2543
	$\bar{\alpha}$	20°		+135°	1371
5 [b]	$\bar{\alpha}, p$	20°	-65°	-60°	~300

[a] Negative when on the opposite side of the beam from the α' detector.

[b] Calibration run to check the singles, $\bar{\alpha}, p$ yields against one another.
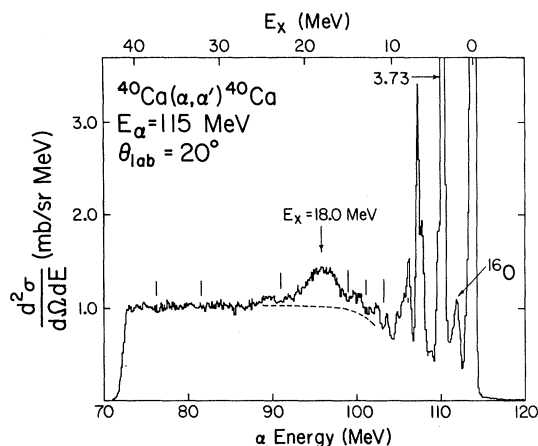
FIG. 3. A ^{40}Ca$(\alpha, \alpha')^{40}$Ca spectrum taken at 20°. The dashed line indicates the empirically determined shape of continuum underlying the GQR.

FIG. 4. (a)–(e) ^{40}Ca$(\alpha, \alpha p)^{39}$K spectrum representing true α-p coincidences. The yield per channel is proportional to the box size (channels having more than 150 counts are represented by square boxes). The intense diagonal band corresponds to events populating the ^{39}K ground state. Several projections of the events into "ordinary" spectra are illustrated and discussed in the text.

distribution. At $E_x \sim 14.0$ MeV there is a group (containing at least two peaks) with a width $\Gamma \sim 1.4$ MeV which has an angular distribution fit very well by $L = 2$ and exhausts $\sim 7\%$ of the $E2$ energy-weighted sum rule (EWSR).[3] The broad peak (the GQR) located at $E_x = 18$ MeV sits on a continuum which is flat at higher excitation but begins to decrease under or just below the GQR where discrete states become prominent. The most pervasive difficulty in analyzing inelastic hadron scattering spectra of the GQR is the determination of the shape and magnitude of this continuum. The continuum shape under the GQR is estimated by smoothly joining the data above and below the GQR. More complete descriptions of the methods used to estimate the continuum shape and the uncertainties involved are given elsewhere.[3] The cross section for excitation of the GQR in ^{40}Ca by 115-MeV α particles at $\bar{\theta}_{lab} = 20°$, averaged over the 5° angular acceptance in the coincidence geometry, was found to be 1.96 ± 0.15 mb/sr. This corresponds to $41 \pm 6\%$ of the $E2$ EWSR. The uncertainty on the cross section is the rms deviation observed in the six measurements made during the coincidence runs, while the uncertainty on the EWSR fraction includes an allowance for $\pm 0.5°$ relative angle error between the data and the DWBA calculation. Errors due to choice of background and target thickness uncertainties have not been included and contribute an additional 25% uncertainty in the cross section. This EWSR fraction is in good agreement with the value obtained earlier from (α, α') (42%; Ref. 3).

A two-dimensional spectrum from the ^{40}Ca$(\alpha, \alpha p)$ ^{39}K reaction is shown in Fig. 4 after subtraction of the accidental coincidences. The kinematic locus for events populating the ^{39}K ground state is ap-
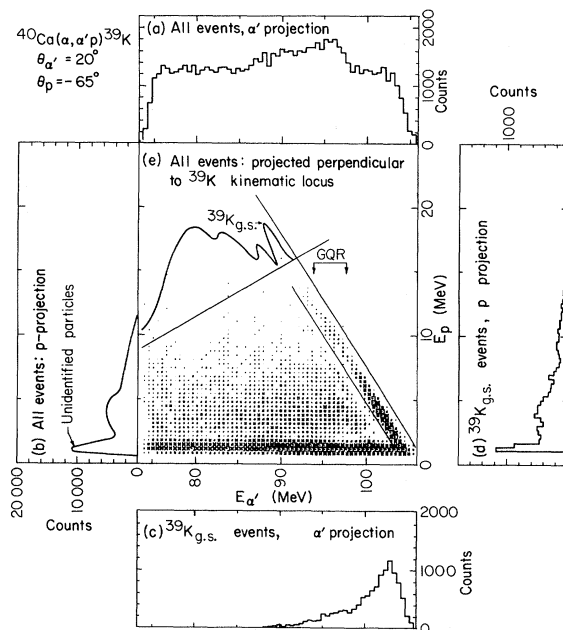
parent. Most of the accidental coincidences fell along lines corresponding to the ground and 3.73-MeV states of ^{40}Ca. The spectrum of accidental coincidences was normalized to the true plus accidental spectrum using the number of events in the elastic peak (all must be accidental coincidences) and the spectra subtracted to leave only the true events. The true to accidental coincidence ratio in the region of interest was $\gtrsim 6$ to 1. To facilitate interpretation of the data several different projections to obtain "ordinary" spectra are desirable and are also illustrated in Fig. 4. The first two [Figs. 4 (a) and (b)] are obtained by projecting all events onto the α' and p axis, respectively, and are the α' and p spectra obtained for all coincidence events. To obtain spectra representing transitions to one final state in ^{39}K or ^{36}Ar, lines are drawn separating events along the appropriate kinematic locus from other events and projections made onto the α' and p axis for events between the lines [Figs. 4 (c) and 4(d)]. Due to the heavy mass of one of the three-body reaction products (^{39}K or ^{36}Ar) relative to the other two, the kinematic loci are almost straight and were approximated by straight lines. For the ground state of ^{39}K and the three observed states of ^{36}Ar the population of the groups

and their separation was such that the lines sep-
arating groups could be reliably located using a
128×128-channel computer printout of the 2D
spectra. For the ^{39}K group at 2.5 MeV, however,
this was not satisfactory. A projection of the
events onto an axis perpendicular to the kinematic
locus [Fig. 4(e)] produces a clear spectrum of the
population of states in the residual nucleus (^{39}K or
^{36}Ar). The limits for events populating ^{39}K in the
2.5-MeV region were obtained by picking points
on this projected spectrum (Fig. 5) representing
the upper and lower limits for this peak and using
the known slope of the kinematic locus to draw the
lines separating this group from the others in the
two-dimensional spectra. Parameters represen-
ting the location of the lines were read into a com-
puter code which searched the event-by-event data
tape (in 2048-×2048-channel resolution) to locate
all events falling between the lines. 1024-channel
spectra representing projections of these events
on each axis (α' and p or α) and along the kine-
matic locus were produced for true and accidental,
accidental only, and true coincidences only and
were stored on magnetic tape for future analysis.
In addition to (or in place of) the lines parallel to
the kinematic loci, horizontal and vertical lines
representing upper and lower limits on α' and α
or p energies were used when necessary. While
the data were taken in 2048-channel resolution for
both axes, compression factors from 2 to 16 were
generally used in displays of the projected spectra
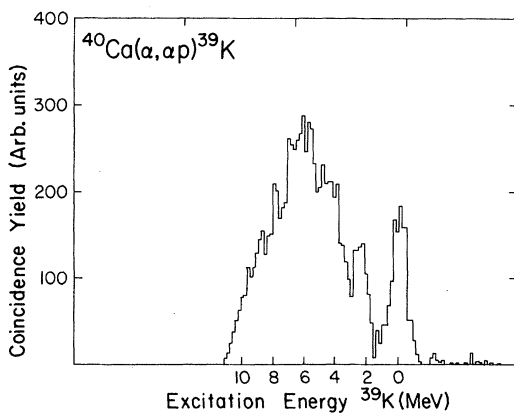to make the features of the data more apparent.

FIG. 5. True coincident events from the ^{40}Ca(α, $\alpha'p$)^{39}K
reaction projected onto an axis perpendicular to kine-
matic loci corresponding to population of states in ^{39}K
[Fig. 4(e)]. Only those events whose α' energy would
correspond to excitation of ^{40}Ca into the GQR region
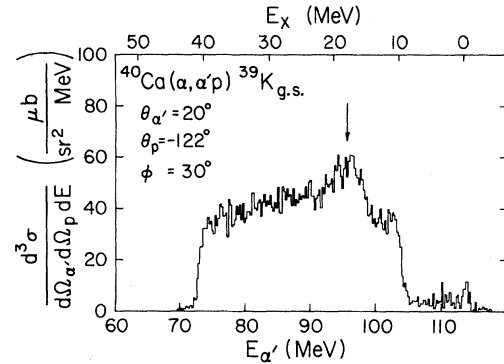(16.4 ≤ E_x ≤ 20.7 MeV) are included.

FIG. 6. Spectra of α particles in coincidence with all
protons (2.5 MeV ≤ E_p ≤ 15 MeV) for one run [Fig. 4(a)].
Accidental coincidences have been subtracted.

A. Proton decay

Proton decay data were obtained at six angles in
the reaction plane and one angle 30° out of the re-
action plane. The two-dimensional spectra are
characterized by events along kinematic loci cor-
responding to ^{39}K left in both the ground state and
a group of states around the first-excited state (the
2.53-, 2.82-, and 3.02-MeV levels were not re-
solved). In all the spectra the group at 2.5 MeV
was populated much less than the ground state
(see Fig. 5), and no higher ^{39}K states could be
positively identified although there was consider-
able decay to that region. Except for the spectrum
obtained with θ_p near the recoil angle (−65°), few
events were seen with proton energies above
10 MeV, although protons with laboratory energies
from 2.5–20 MeV (θ_p = −65°, −90°), 2.5–15 MeV
(θ_p = −122°, −125°, −150°), and 2.5–12 MeV (θ_p
= 145°, 120°) would be recorded in the spectra.

A projection of all coincidences on the α' axis
is shown in Fig. 6. The spectrum looks much like
an ($\alpha'\alpha$) singles spectrum for α' energies cor-
responding to ^{40}Ca excitation above 10–11 MeV.
The peak at 14 MeV seems relatively weaker than
in the singles data, and the GQR sits on a back-
ground which is approximately flat at higher excit-
ation energies. There is little difference in the
spectra at the seven angles taken. The cross
sections are about 45 μb/sr^2 MeV in the flat re-
gion which corresponds to about 52% of the avail-
able decay cross section, if the decay is assumed
to be isotropic. The angular correlation for the
GQR peak remaining after subtracting a background
similar in shape to that used in the singles data[3]
(justified primarily by the similarities in the co-
incidence and singles spectra) is essentially iso-
tropic and the value of Γ_p/Γ obtained is $0.70^{+0.15}_{-0.20}$.
The spectra projected onto the proton axis (Fig.

7) have the characteristics of an evaporation spectrum, peaking in the region of 4 MeV (which is approximately the $p+{}^{39}$K Coulomb barrier height) and decreasing approximately exponentially at higher energies. Below $E_{p(\text{lab})} \approx 2.5$ MeV the protons were stopped in the ΔE detector, and the events were rejected. An estimate of the number of events lost due to the proton detector low-energy cutoff was made assuming that the shape of the proton spectrum at energies in the vicinity of the cutoff is determined primarily by the Coulomb penetrability. The yield of low-energy protons was approximated as $Y = KP(E_p)\rho_{39K}(E_x)$ where K is an arbitrary constant determined by normalization to the data, $P(E_p)$ is the Coulomb penetrability in the $p+{}^{39}$K channel, and $\rho_{39K}(E_x)$ is the density of states in ^{39}K to which the decay is proceeding. The density of states was approximated[12] as $\rho(E) = C/E\,[\exp(BE^{1/2})]$ where the parameters were estimated from the known levels in ^{39}K. This calculation of the low-energy proton spectrum is shown superimposed on the data in Fig. 7. While this estimate is relatively crude, it does reproduce the shape of the spectrum reasonably well in the vicinity of the cutoff and probably provides an adequate estimate of the proton events missed; these range from 5% to 25% of the yield, depending on angle.

A projection of all events whose α' energy corresponds to ^{40}Ca excited in the GQR region (16.4 MeV $\lesssim E_x \lesssim 20.7$ MeV) onto an axis perpendicular to the ^{39}K ground state kinematic locus is shown in Fig. 5. The ^{39}K ground state and the group of states at 2.5 MeV are populated in the proton decay, but the bulk of the decay proceeds to the 5–8-MeV region
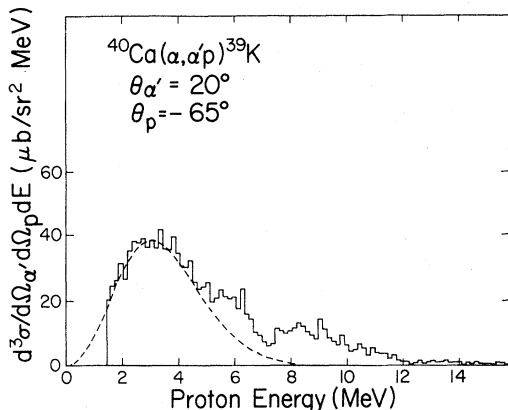
of excitation in ^{39}K. The falloff at higher ^{39}K excitation energy is due to the combined effects of the Coulomb barrier for the decay protons and the detector cutoff. In order to establish whether the decay observed to the ground and first-excited states of ^{39}K is due to the GQR or the underlying continuum, projections onto the α' axis were made for events lying along the kinematic loci for transitions to these states. Examples of these spectra are shown in Fig. 8. In most of the spectra there is a peak at ^{40}Ca $E_x \sim 18$ MeV with approximately the width of the GQR as well as a peak in the ^{40}Ca $E_x \sim 12$–14-MeV region. In contrast to the singles spectra and the spectra of all decay particles, there is little yield at excitation energies above the peak, indicating that the continuum observed above the peak does not decay to the lower states in ^{39}K. In order to extract yields for the GQR a power series "background" was fitted to the data on either side of the peak, and after subtraction of this background the yield corresponding to excitation energies between 15.0 and 22.7 MeV was summed. The resulting correlation functions, after center of mass and solid angle corrections, are shown in Fig. 9. The upper error bar was ob-
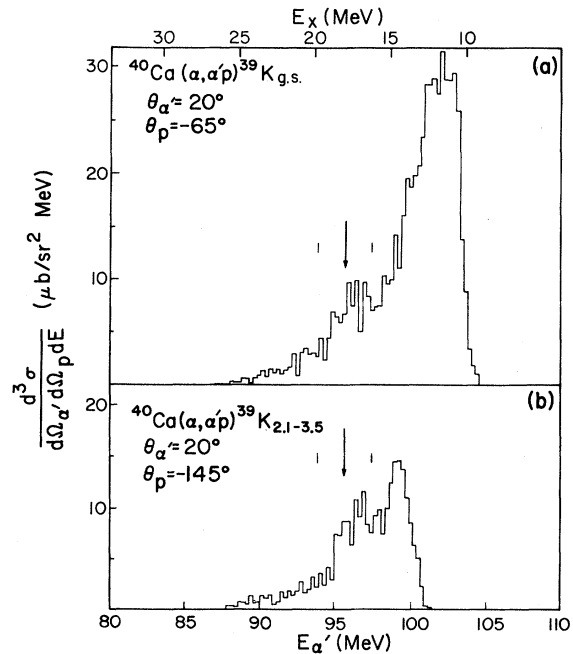
FIG. 7. A spectrum of protons in coincidence with α particles whose energy corresponds to excitation of ^{40}Ca between 16.4–20.7 MeV. The proton energy is given in the ^{39}K $+p$ center of mass system. The dashed curve represents a simple estimate of the shape of the spectrum from level density and penetrability considerations and has been arbitrarily normalized to the data.

FIG. 8. (a) Spectra of α particles in coincidence with protons leaving ^{39}K in the ground state. (b) Spectra of α particles in coincidence with protons leaving ^{39}K excited around 2.5 MeV. Accidental coincidences have been subtracted. These correspond to the projection in Fig. 4(c). The arrow indicates the position and the lines the width of the GQR (as observed in the singles spectrum).
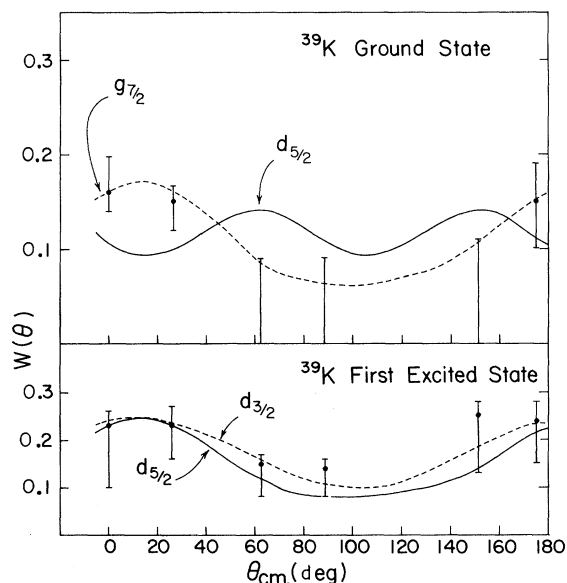
FIG. 9. Angular correlation functions for proton decay of the GQR. The curves are the result of DWBA calculations and the experimental points are the values extracted from the coincidence measurement. The angle is with respect to the ^{40}Ca recoil direction. The proton partial waves are indicated.

tained by assuming essentially no background in the coincidence data, while the lower error bar represents about the highest practical background choice. The statistical errors are considerably smaller. At angles where only upper limits are shown, no peak was observed at the GQR position. The correlations are somewhat similar, both peaking in the vicinity of 0° relative to the ^{39}K + p c.m. recoil direction. The ground-state correlation is certainly not isotropic since the GQR is not apparent at three angles but is present at the other three. The correlation for decay to the first excited state is also not isotropic unless one is content with accepting the upper limits at some angles and the lower limits at others, but this would represent very different assumptions about the background. The lack of isotropy adds to the evidence that this is not a monopole state. The centroid energies and rms widths (see Ref. 3) for

the GQR peak obtained from the various sets of coincidence data are compared with those derived from the singles data in Table II. Generally the results agree within the errors, although the centroid energy obtained for decay to the ground and first-excited states are systematically lower than the others. This is likely due to the opening up of competing p and n channels in the upper region of the GQR causing a reduction in the decay to these channels. The rms widths obtained are extremely sensitive to the choice of background, hence the uncertainties are quite large.

B. α decay

Unlike the coincidence proton spectra, which had the same qualitative appearance at all the angle pairs studied, the character of the coincidence α spectra changed markedly as the $\bar{\alpha}$ detector changed angles. Figure 10 shows the spectrum measured with the α' detector at 20° and the $\bar{\alpha}$ detector at $-82°$ (on the opposite side of the beam). Events with $\bar{\alpha}$ energies up to 26 MeV are seen distributed along the kinematic loci for leaving ^{36}Ar in its ground state, first-excited state (2⁺) at 1.97 MeV, and the next group of states around 4 MeV. At α' energies below these kinematic loci the majority of the events occur with $\bar{\alpha}$ energies below 10 MeV. The spectrum measured with the $\bar{\alpha}$ detector at $-60°$ in the laboratory showed a conspicuous peaking of events centered around $E_\alpha = 20$ MeV, presumably due to knockout. On the other hand, the spectra measured with the $\bar{\alpha}$ detector in the backward hemisphere had few events with $\bar{\alpha}$ energies above 10 MeV. At $\theta_{\bar{\alpha}} = 120°$ and 135° many of the $\bar{\alpha}$'s of interest have laboratory energies less than the 5.5 MeV needed to penetrate into the E detector. Hence, at these two angles the spectra of events for particles stopped in the ΔE detector were also taken. The stopped particles were in the energy range between 1.3 and 5.5 MeV. Very few particles other than α particles and protons have been identified; however, protons above 1.4 MeV would penetrate into the E detector. Therefore, most of the observed particles must be α particles. Further, the spectrum of stopped particles joins smoothly with the

TABLE II. Centroid energies and rms widths obtained for the GQR.

	Previous [a]	Singles [b]	All p	^{39}K(g.s.)	^{39}K(1st)
E_x (MeV)	18.0±0.2	18.1±0.3	17.9±0.4	17.5±0.4	17.4±0.4
Γ (MeV)	3.5±0.3	4.0±0.3	4.5±0.4	4.1±0.5	3.9±0.5

[a] Reference 3.

[b] Taken at $\theta_{lab} = 20°$ with the large coincidence solid angle.
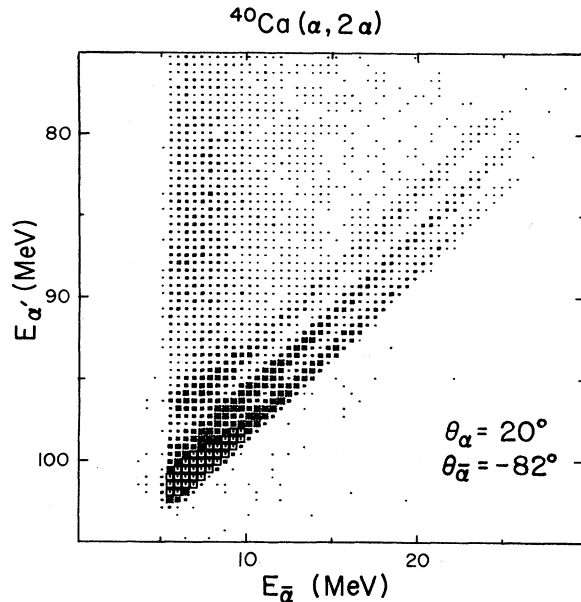
^{40}Ca $(\alpha, 2\alpha)$

FIG. 10. ^{40}Ca$(\alpha, 2\alpha)^{36}$Ar spectrum for true $\alpha'-\bar{\alpha}$ co-incidence events. The yield per channel is proportional to the box size (channels having more than 100 counts are represented by square boxes). The three diagonal bands represent events leaving ^{36}Ar in its ground, 1.97-, and 4.3-MeV states.

identified α particles.

The spectra projected on the α' axis are shown in Fig. 11. These spectra show an increasing yield at forward angles with a large knockout peak which dominates the spectrum measured with the $\bar{\alpha}$ detector at $-60°$. With the $\bar{\alpha}$ detector $22°$ farther back in angle, the spectrum rises monotonically with increasing α' energy and has a peaking of events near the kinematic threshold for $\bar{\alpha}$ emission ($E_{\alpha'} = 106.6$ MeV). The spectra measured in the backward hemisphere have nearly uniform yield over the entire excitation range studied except for a peak around $E_{\alpha'} = 100$ MeV. The total GQR decay into the α channel might be deduced from the spectra shown in Fig. 11 by separating the observed yield into a part due to the continuum and a part due to the GQR. Such an analysis was performed, yielding a value for Γ_α/Γ of $0.21^{+0.05}_{-0.15}$ for the residual events above the continuum in the GQR region. However, the centroid varied by more than 2 MeV between the different spectra (even though the analysis region was fixed to be $15.0 \leq E_x \leq 22.7$ MeV) suggesting that this cannot be reliably associated with GQR decay.

In order to ascertain the decay to the low-lying states of ^{36}Ar, events lying along the kinematic loci for decay to those states were projected onto the α' axis. These projections for the coincidence
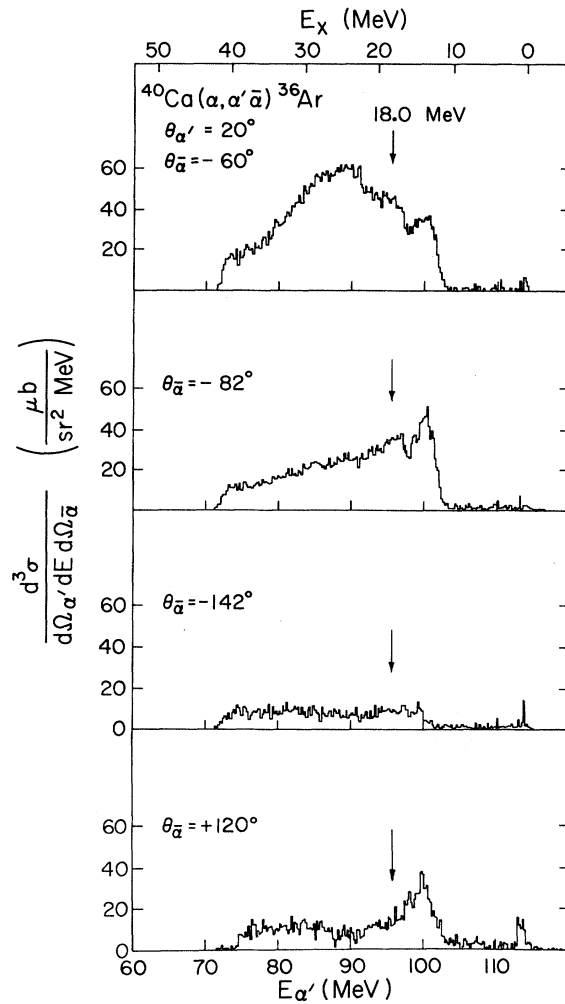

FIG. 11. Projections of the total true ^{40}Ca$(\alpha, 2\alpha)$ coincidence spectra measured at several angles onto the α' axis [Fig. 4(a)]. The top spectrum was measured near the quasifree angle and shows a large knockout contribution. The arrow indicates the position of the GQR.

spectrum measured with $\theta_{\bar\alpha} = -120°$ are shown in Fig. 12. The peak of the α_0 events lies at about 14 MeV, a feature which persists at all of the angles measured, while there is only weak evidence for the 12-MeV group or the GQR peak. An angular correlation for α_0 decay of the 14-MeV group obtained by fitting the spectra assuming groups at 12 and 14 MeV and a continuous "background" is shown in Fig. 13. The striking correlation is characteristic of decay of a $J^\pi = 2^+$ state (as will be discussed in the next section). The yield corresponds to $\Gamma_{\alpha_0}/\Gamma \sim 0.9 \pm 0.2$ for the group at $E_x \approx 13.9$ MeV with $\Gamma \approx 1.4$ MeV. Due to the proximity of the $\bar\alpha$ detector low-energy threshold, no meaningful correlation could be extracted for the 12-MeV group.

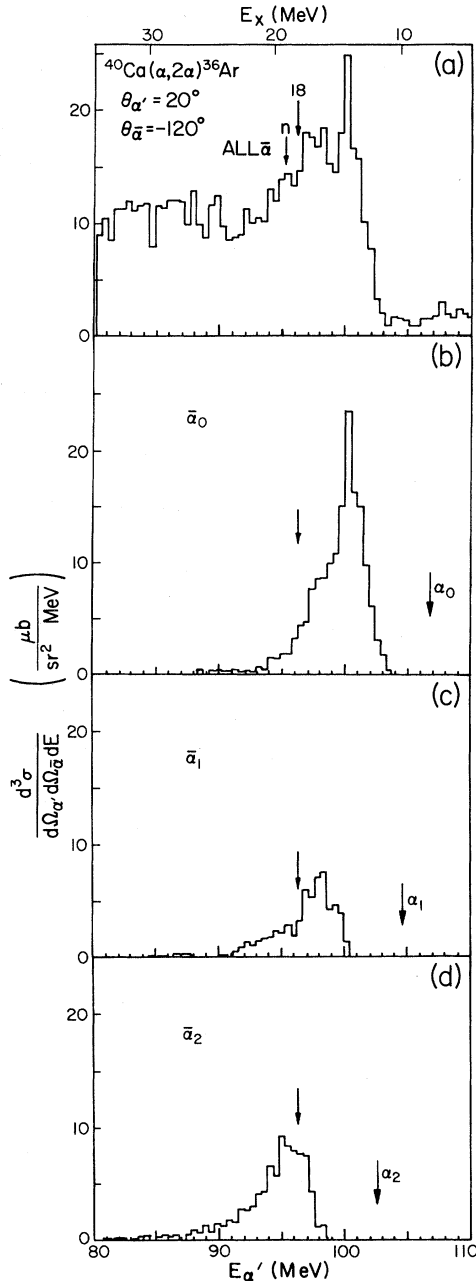The correlation for a 2^+ state is strongly peaked

E_x (MeV)

^{40}Ca$(\alpha,2\alpha)^{36}$Ar

$\theta_{\alpha'} = 20°$

$\theta_{\bar{\alpha}} = -120°$

ALL $\bar{\alpha}$

(a)

18

n

(b)

$\bar{\alpha}_0$

α_0

(c)

$\bar{\alpha}_1$

α_1

(d)

$\bar{\alpha}_2$

α_2

$\left(\dfrac{\mu b}{sr^2 \, MeV}\right)$

$\dfrac{d^3\sigma}{d\Omega_{\alpha'} d\Omega_{\bar{\alpha}} dE}$

$E_{\alpha'}$ (MeV)

FIG. 12. Decomposition of the ^{40}Ca$(\alpha,2\alpha)$ coincidence spectrum projected onto the $E_{\alpha'}$ axis. The total true yield is shown in (a). The projection of events leaving ^{36}Ar in its ground state (b), first-excited state (c), and in states around $E_x = 4$ MeV (d) are also shown. These projections are the type in [Fig. 4(c)]. The GQR position, n threshold, and α decay thresholds are indicated.

close to 0° and 180° in the recoil system (as seen for the 14-MeV group). Due to the relatively large direct contribution to the spectra near 0° recoil, the most sensitive measure of GQR decay would be at $\theta_{c.m.} \sim 180°$. While enhancement of the

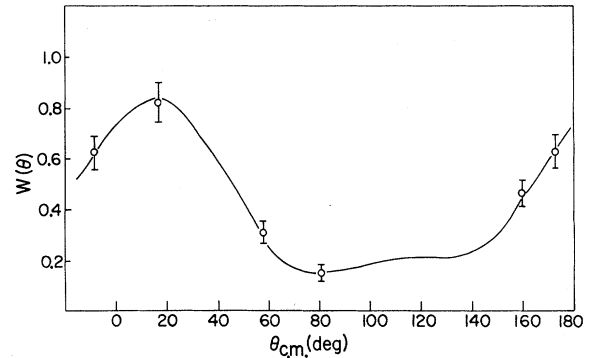$W(\theta)$

$\theta_{c.m.}$ (deg)

FIG. 13. Angular correlation function for α decay of the 13.9-MeV state in ^{40}Ca to the ground state of ^{36}Ar. The errors shown include an estimate of the uncertainty in extracting the peak yield. The solid curve is a theoretical calculation for decay of a $J^\pi = 2^+$ state performed as described in the text.

$J^\pi = 2^+$ 14-MeV group is evident in the spectrum taken at $\theta_{\bar{\alpha}} = 120°$ ($\theta_{c.m.} \sim 175°$) the GQR peak is conspicuously absent (this is apparent even in the spectrum for all α's shown in Fig. 11). If Γ_{α_0} is assumed to be independent of energy for the GQR an upper limit of $\Gamma_{\alpha_0}/\Gamma < 0.06$ can be established.

The spectra for decay to the 2^+ state at 2 MeV in ^{36}Ar showed a small decay from the 14-MeV state but there was no peaking of events in the region of the GQR. An upper limit for this decay branch of $\Gamma_{\alpha_1}/\Gamma \lesssim 0.1$ was established. The peak for the $\bar{\alpha}_2$ decay does fall in the GQR region and would correspond to $0.24^{+0.03}_{-0.06}$ of the decay of the GQR. However, the centroid of the peak is ~ 1 MeV above the GQR. The decay to this state is inhibited by the Coulomb barrier ($V_C \simeq 7.7$ MeV) on the high α' energy side, while increased competition from the neutron channel which opens at $E_{\alpha'} = 94.9$ MeV decreases the yield on the low α' energy side. Thus it is reasonable to ascribe the observed peaking in the $\bar{\alpha}_2$ channel to the above two effects rather than a preferential decay of the GQR through this channel.

Having concluded that there is no evidence for α decay of the GQR, it is of interest to deduce the total α decay width for various regions of the α' spectrum. The cross section averaged over the region of the GQR ($15.0 \le E_x \le 22.7$ MeV), for the angles where there was no direct contribution was about 12 μb/sr^2 MeV. If this is taken to represent an isotropic component of the decay, then this contributes approximately 12% of the yield in this region of the singles spectrum. The contribution to the α' singles spectrum from the direct knockout process, which dominates the coincidence spectra at the two angles near the recoil angle, may also be estimated. In order to obtain the

contribution from this process the complete angular correlation must be known, and little such information is available. Recently, however, Sherman[13] has studied the correlation in $(\alpha, 2\alpha)$ reactions with targets from C to Zn using detectors both at symmetric angles and (for ^{12}C and ^{16}O) at asymmetric angles with one detector fixed at $42°$ in the lab. In the latter case, the measured differential cross sections for both targets were nearly constant when the second α detector is moved over an angular range of $15°$ but dropped quickly at larger angles. Since this angular spread is probably due to the Fermi motion of the α at the instant of knockout, the angular correlation should have azimuthal symmetry about the quasifree angle. If one takes these results also to be valid for ^{40}Ca and assumes the knocked-out α particles are uniformly distributed over a cone with a half opening angle of $15°$, the contribution to the singles spectrum from this process can be estimated. Utilizing the cross section observed for the knockout process with the detector at $-60°$, the predicted contribution to the singles cross section would represent about 4% of the yield in the region of the GQR peak. From this estimate the direct α knockout contribution to the α' singles spectrum appears to be negligible.

In the excitation region above the GQR, the α' coincidence spectra are structureless, except for the direct contribution in the spectrum of $\theta_{\overline{\alpha}} = -60°$. Excluding this spectrum, the average differential cross section for the region from $E_{\alpha'} = 76$ to 82 MeV for the other spectra is 14 μb/sr^2 MeV. Assuming this average to represent isotropic decay, 17% of the decay of this region is by α emission.

In the region of excitation below the GQR, just above the α particle threshold, considerable

peaking is seen in the coincidence spectra. The spectra in this region were cut off by the $\overline{\alpha}$ detector threshold and thus a meaningful analysis can be done only for the 2-MeV region $E_{\alpha'} = 98$ to to 100 MeV. The decay of the 14-MeV $J^\pi = 2^+$ state accounts for ~ 20% of the singles events in this region while an additional ~9% represent "other" decays into the α channel. Thus a total of ~29% of the decay of this region is by α emission.

DISCUSSION

A summary of the observed decay branches is given in Table III. In addition to the p and α decays discussed in the previous section, a column has been added which represents decay observed when taking the proton data for which there was no particle identification because the decay particles stopped in the 50-μ ΔE detector. Due to the way the windows were set, only particles with energies between ~1.3 and 2.5 MeV would contribute to this; however, a substantial portion of the decay resulted in particles in this range.

One feature this table makes apparent is that not all of the spectrum is accounted for in the observed decay, even for the 10.8–12.7- and 12.7–15.0-MeV regions where only proton and α channels are open (neglecting the γ channel). In the α channel, decays resulting in 2.5 $\leq E_\alpha \leq 5.5$ MeV would not be seen due to the ΔE detector thickness in the $\overline{\alpha}$ stacks, and the upper limit determined by window settings in the unidentified events (except at $\theta_{\overline{\alpha}} = 120°, 135°$). For the region of excitation from 10.8–12.7 MeV where E_α^{max}(c.m.) is ~5.7 MeV, 70% of the decay is accounted for in the proton and "other" decay, leaving 30% for the α channel, which is qualitatively reasonable. For the 12.7–15.0-MeV region

TABLE III. Decay fractions observed for various excitation regions of ^{40}Ca. The data were not (and cannot be) restricted only to events where the ^{40}Ca was first excited and then decayed. The excitation range given was determined by assuming an (α, α') reaction first exciting ^{40}Ca, and identifying excitation energies with α' energies.

E_x	p_0	p_1 [a]	All p [b]	α_0	α_1	α_2 [c]	All α [d]	Other [e]	Total
GQR (15–22 MeV) [f]	$0.08^{+0.05}_{-0.03}$	$0.22^{+0.05}_{-0.08}$	$0.70^{+0.15}_{-0.20}$	<0.06	<0.10	$(0.24^{+0.03}_{-0.06})$ [g]	$(0.21^{+0.05}_{-0.15})$ [g]		
10.8–12.7 MeV			0.38 ± 0.04					0.32 ± 0.04	0.70 ± 0.07
12.7–15 MeV			0.37 ± 0.04				0.29 ± 0.04	0.17 ± 0.02	0.83 ± 0.08
15–22.7 MeV			0.47 ± 0.05				$0.15^{+0.10}_{-0.04}$	0.17 ± 0.02	$0.79^{+0.11}_{-0.08}$
31–35 MeV			0.52 ± 0.05				$0.17^{+0.10}_{-0.06}$	0.17 ± 0.02	$0.86^{+0.12}_{-0.09}$

[a] The $2.2 \leq E_x \leq 3.5$ MeV group of ^{39}K states around 2.5 MeV were not resolved.

[b] 2.5 MeV $\leq E_p \leq 20$ MeV.

[c] The group of ^{36}Ar states around 4.3 MeV were not resolved.

[d] 5.5 MeV $\leq E_\alpha \leq 25$ MeV.

[e] Events which stopped in the 50-μm ΔE detectors and hence were not identified ($1.3 \leq E \leq 2.5$ MeV).

[f] The decays given in this row are relative to the GQR yield only. A continuum "background" has been subtracted.

[g] These are probably not due to the GQR (see text).

where E_α^{max}(c.m.) is ~8.0 MeV (from the upper end of the region; for the lower end it is again 5.7 MeV), 29% of the decay is unobserved, again a reasonable fraction. For the other regions, the competing neutron channel is open, so that one would not expect to observe all of the decay. The relatively large fraction observed in the high excitation region, where one might expect the p and n decay probabilities to be about equal, is likely due to multiparticle decays (such as $2p$, $p+\alpha$, 2α) which result in double counting of events and would cause the extracted decay fractions to be too high.

The α'-p and α'-$\bar\alpha$ angular correlations depend on the polarization given to the decaying GQR in the (α, α') reaction and on the properties of the subsequent p or $\bar\alpha$ decay to the final state. In the following it is assumed that the GQR is excited in a one-step interaction with the incident α particle and the subsequent behavior of the GQR is uninfluenced by the α proximity. In order to describe the initial polarization of the GQR a computer code was written which constructs its density matrix in the conventional manner[14] from the reaction amplitudes calculated by the DWBA code DWUCK.[15] From the density matrix the correlation function $W(\theta, \phi)$ is calculated for a decay characterized by $\vec{l}$, $\vec{s}$, and $\vec{j}$ to a final state of spin J. The decay particle may be a proton, a neutron, an α particle, or a γ ray. In combining decays to a given final state with different lsj values it is assumed that no interference occurs. The code was checked by calculating $W(\theta, \phi)$ for several reactions in the plane wave limit where the correlation functions are simple. The calculation for decay of a $J^\pi = 2^+$ state located at 14 MeV to the ^{36}Ar 0^+ ground state, shown superimposed on the data in Fig. 13, is not very different from the plane wave result ($|Y_{20}(\theta)|^2$ with θ measured relative to the recoil direction). The agreement with the data is excellent, confirming the previous assignment[3] for this state. This state exhausts[3] only ~7% of the EWSR, but decays almost entirely by α_0 emission. In contrast, the GQR which has roughly six times the singles cross section (~42% of $E2$ EWSR) and a very similar theoretical angular correlation, is not at all apparent in the coincidence spectra. Thus, an upper limit for α_0 decay of the GQR of $\Gamma_{\alpha_0}/\Gamma \leq 0.06$ was established. The ^{36}Ar(α, γ) results of Branford[8] are in agreement with the ground-state α decay measured in the present experiment. Figure 14 shows the $\sigma^{E2}(\alpha, \gamma_0)$ cross section deduced by Branford. The cross section peaks around 14 MeV and in the GQR region has a fluctuating cross section with a mean value ~0.53 μb. From this value and assuming an $E2$ resonance exhausting 42% of the sum rule, it is estimated that the decay fraction through the α_0 chan-
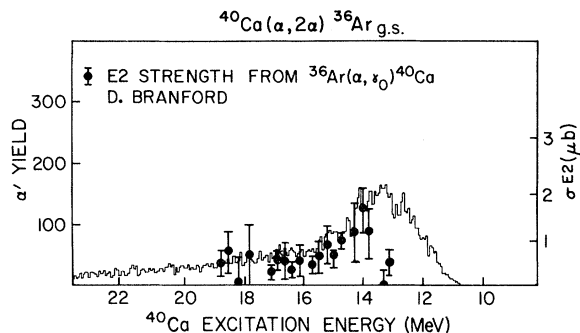

FIG. 14. Projection of ^{40}Ca$(\alpha, 2\alpha)^{36}$Ar(g.s.) events onto the α' axis [Fig. 4(c)] which has been labeled on a ^{40}Ca excitation energy scale. These events were measured with the $\bar\alpha$ detector at $\theta = -120°$. Also plotted are $E2$ cross sections deduced from ^{36}Ar$(\alpha, \gamma_0)^{40}$Ca measurements of Branford (Ref. 8).

nel is ~0.06 which is in agreement with the limit established in the present work. Also plotted in Fig. 14 is the spectrum of ground-state decay (α_0) from the GQR. It is seen that the shapes of the data are very similar in the region of the 2^+ state at 14 MeV and the GQR.

To obtain the relevant configurations for the giant quadrupole and monopole states, a simple model of a coherent sum of $2\hbar\omega$ 1p-1h states was assumed. Wave function amplitudes obtained for both states using the random phase approximation (RPA) are shown in Table IV.[16] The levels in ^{39}K (Table IV) available for proton decay are the $d_{3/2}$ ground state, the $s_{1/2}$ state at 2.5 MeV, and a group of several $d_{5/2}$ states from 5–6 MeV as well as several states of more complicated configurations. Pickup reactions[18] on ^{40}Ca have shown that these states are reasonably well represented by single holes in the $d_{3/2}$, $s_{1/2}$, and $d_{5/2}$ orbits, respectively. Utilizing the method described above, α-p angular correlations have been calculated for direct decay of the GQR to the ^{39}K ground and first-excited states through both the expected dominant partial waves ($g_{7/2}$ for ground state and $d_{5/2}$ for the first-excited state) and a second, but considerably weaker, component. These calculations averaged over the angular openings of the detectors are shown superimposed on the data in Fig. 9. The agreement with the data is quite good although one certainly cannot distinguish between the $d_{5/2}$, $d_{3/2}$ partial waves in the decay to the $s_{1/2}$ state. As expected the $g_{7/2}$ partial wave is clearly favored over the $d_{5/2}$ partial wave in decay to the $d_{3/2}$ state.

Exclusive of penetration factors the relative population of these states by direct proton decay (or ^{39}Ca states by neutron decay) of the giant resonance should be given by the ratio of the squares of the amplitudes of the configurations containing

TABLE IV. Dominant particle-hole configurations of the isoscalar quadrupole and monopole states of ^{40}Ca.

	$(0f_{5/2})(0p_{1/2})^{-1}$	$(0f_{7/2})(0p_{3/2})^{-1}$	Quadrupole[a] $(1d_{5/2})(1s_{1/2})^{-1}$	$(0g_{7/2})(0d_{3/2})^{-1}$	$(0g_{9/2})(0d_{5/2})^{-1}$
Proton	1%	6%	2%	8%	37%
Neutron	1%	5%	2%	11%	25%
	$(1p_{1/2})(0p_{1/2})^{-1}$	$(1p_{3/2})(0p_{3/2})^{-1}$	Monopole $(2s_{1/2})(1s_{1/2})^{-1}$	$(1d_{3/2})(0d_{3/2})^{-1}$	$(1d_{5/2})(0d_{5/2})^{-1}$
Proton	5%	10%	8%	11%	16%
Neutron	5%	10%	8%	11%	16%

[a]These results are in reasonable agreement with a similar calculation done by Zamick (Ref. 17).

$d_{3/2}$, $s_{1/2}$, and $d_{5/2}$ hole components, respectively. The proton decay of the dominant components of the quadrupole resonance involves g wave ($d_{3/2}^{-1}$ and $d_{5/2}^{-1}$ states) and d wave ($s_{1/2}^{-1}$ state) emission and, due to the low proton energies involved, will be dominated by penetrability factors for the different states. Table V lists the energies, partial waves, and penetrability factors for the applicable decay modes of the resonance. Included are the decay parameters predicted for the ground-state neutron decay. This is the only energetically allowed neutron decay of the GQR. The small penetrability for this low-energy g wave makes the decay negligible. Similarly a large hindrance of the decay to the $d_{5/2}^{-1}$ proton configuration results from the low-energy g wave proton decay, and the decay on this basis should be dominated by a transition to the $(d_{3/2})^{-1}$ ground state in ^{39}K. (For a monopole, approximately equal decay to the $d_{3/2}$ and $s_{1/2}$ hole states is predicted.) The experimental data on the other hand show -8% and -22% of the total decay proceeding to the $d_{3/2}$ and $s_{1/2}$ hole states in ^{39}K, with $\sim40\%$ to higher excitation. The relatively poor agreement with the theory suggests possibly that the

simple estimates of the relative strengths of these small components of the GQR wave function may not be accurate. A second more likely explanation, however, is that the GQR mixes strongly with more complicated underlying 2^+ states which subsequently proton decay. These decays would not favor the simple configurations and would enhance the yield to the higher excitation region of ^{39}K, where many complicated states are available. The coincidence spectra projected to show the yield as a function of ^{39}K excitation energy (see Fig. 5) support this explanation. It is seen that, except for the ground and first-excited state, the yield rises more or less smoothly as excitation energy increases from the region around the first-excited state to peak and begin decreasing where the Coulomb barrier for proton emission (and the detector cutoff) reduces the proton yield.

From these results one can in part understand why the $E2$ strength measured in proton capture reactions falls below the sum rule estimate. The ground-state proton decay branch for the GDR is $\Gamma_{p_0}^D/\Gamma \sim 0.20$,[9,11] whereas from Table III for the GQR $\Gamma_{p_0}^Q/\Gamma = 0.08_{-0.03}^{+0.05}$. Based on the sum rules, it was estimated that the ratio $E2/E1$ of strengths

TABLE V. ^{40}Ca GQR decay branches.

Branch	Config.[b]	E_p (MeV)	P_l[c]	Γ[a] (MeV)	Γ/Γ_t^{theory}	Γ/Γ_t^{exp}
p_0	$(g_{7/2})(d_{3/2})^{-1}$	9.67	0.70	0.189	0.054	$0.08_{-0.03}^{+0.05}$
p_1	$(d_{5/2})(s_{1/2})^{-1}$	7.1	1.50	0.101	0.029	$0.22_{-0.08}^{+0.05}$
p_2	$(g_{9/2})(d_{5/2})^{-1}$	4.4	0.011	0.014	0.004	
n_0	$(g_{7/2})(d_{3/2})^{-1}$	2.37	0.025	0.009	0.003	

[a]$\Gamma = 2P_l\gamma^2$, where γ^2 is taken as the Wigner limit (~1.69 MeV) times the wave function fraction from the RPA (Table IV).
[b]Major components from the RPA wave function (Table IV).
[c]Penetrabilities from the tables of Marion (Ref. 19).
[d]$\Gamma_t = 3.5$ MeV; this is the width measured in (α, α') (Ref. 3).

was 0.033. In proton capture the measured ratio would be only ~0.013 ± 0.007 in strength and ~0.11 ± 0.04 in amplitude. However, even at this level, through interference with the strong $E1$ strength, the $E2$ strength might be seen in the angular distributions of the capture γ rays. The absence of such evidence in the capture experiment[9] may be due to unfavorable relative phases in the γ decay.

These results are generally in disagreement with the conclusions drawn by Moalem $et\ al.$[20] who performed a similar experiment exciting the ^{40}Ca GQR with a ^{3}He beam. Their data look qualitatively similar to the present work (except with much poorer statistics) and at most angles neither their proton nor α decay spectra show a clear GQR peak. Nevertheless, with their choice of background and utilizing a two-peak fit, they extract GQR yields which are not inconsistent with their data. In so doing they find a GQR decay to the ^{36}Ar ground and first-excited states, whereas the present data, which have much better statistical accuracy, show no peaking which can be associated with the GQR. It is clear that their data are insufficient to permit separation of the GQR peak from the continuum, particularly for decays to individual states in the residual nucleus. Additionally, no account has been taken of the direct knockout processes which could affect the α decay data dramatically. Some other features of their work are unclear, such as how they obtain any α_2 decay fraction for the 13.5–15.6-MeV E_x region, where the maximum α energy (including recoil) is considerably less than their low-energy cutoff. In summary, it is unfortunate that statistical uncertainties are too large in their work to allow a meaningful comparison with the results of the present investigation.

CONCLUSIONS

Proton and α decay of ^{40}Ca* was measured in coincidence with inelastic α particles exciting the nucleus. The results are summarized in Fig. 15. The GQR was found to decay $70^{+15}_{-20}\%$ of the time by proton emission, with $\Gamma_{p_0}/\Gamma \sim 0.08^{+0.05}_{-0.03}$ and $\Gamma_{p_1}/\Gamma \sim 0.22^{+0.05}_{-0.08}$ while the remainder of the decay proceeded to the higher excitation region in ^{39}K. No α_0 decay which could be definitively attributed to the GQR was seen. However, the state at $E_x \approx 13.9$ MeV in ^{40}Ca was seen to decay principally to the ^{36}Ar ground state $\Gamma_{\alpha_0}/\Gamma \approx 0.9 \pm 0.2$ and the measured angular correlation is fit very nicely assuming $J^\pi = 2^+$. The angular correlations ob-
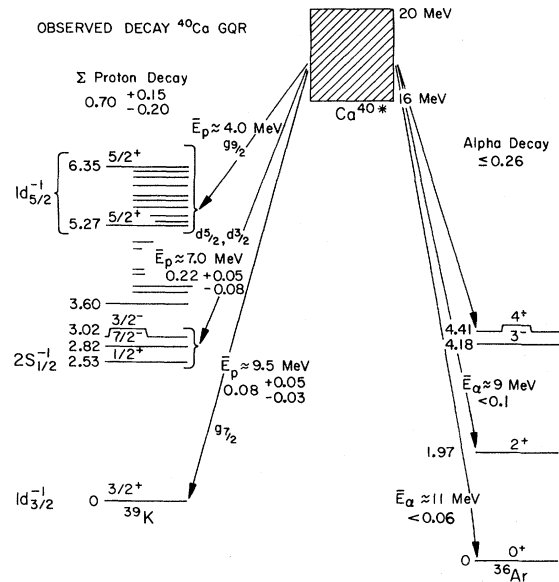

FIG. 15. Summary of the observed charge-particle decay branches of the GQR.

tained for decay to the ^{39}K ground and first-excited states are in good agreement with theoretical predictions for GQR decay and are not consistent with the isotropic decay expected for a monopole state. The relative proton branching is not in agreement with that expected from the direct decay of a simple GQR wave function and suggests there is considerable decay of the GQR into more complicated configurations before particle emission.

Utilizing the observed decay fractions and the known properties of the GDR at the peak of the GQR, $\sigma(E2)/\sigma(E1)$ in proton capture should be ~$0.013^{+0.010}_{-0.007}$, while the $E2/E1$ amplitude ratio would be ~0.11 ± 0.04. At this level one might expect the $E2$ strength to be detectable in the angular distribution. The observed ground-state α_0 decay is consistent with the ^{36}Ar(α, γ) results with considerable strength around 14 MeV but no peaking in the region of the GQR.

*On leave from Physics Department, Indiana University, Bloomington, Indiana.

†Supported in part by the National Science Foundation and the Robert A. Welch Foundation.

[1] R. Pitthan and Th. Walcher, Phys. Lett. 36B, 563 (1971); S. Fukuda and Y. Torizuka, Phys. Rev. Lett. 29, 1109 (1972); F. R. Buskirk, H.-D. Gräf, R. Pitthan, H. Theissen, O. Titze, and Th. Walcher, Phys. Lett. 42B, 194 (1972); M. Nagao and Y. Torizuka, Phys. Rev. Lett. 30, 1068 (1973).

[2] M. B. Lewis and F. E. Bertrand, Nucl. Phys. A196, 337 (1972); A. Moalem, W. Benenson, and G. M. Crawley, Phys. Rev. Lett. 31, 482 (1973).

[3] D. H. Youngblood, J. M. Moss, C. M. Rozsa, J. D. Bronson, A. D. Bacher, and D. R. Brown, Phys. Rev. C 13, 994 (1976).

[4] C. C. Chang, F. E. Bertrand, and D. C. Kocher, Phys. Rev. Lett. 34, 221 (1975).

[5] J. Arvieux, M. Buenerd, A. J. Cole, P. DeSaintignon, G. Perrin, and D. J. Horen, Nucl. Phys. A247, 238 (1975).

[6] L. Meyer-Schützmeister, W. Wharton, P. Debevec, R. E. Segel, and K. Raghunathan, Bull. Am. Phys. Soc. 20, 565 (1975).

[7] J. M. Moss, C. M. Rozsa, D. H. Youngblood, J. D. Bronson, and A. D. Bacher, Phys. Rev. Lett. 34, 748 (1975).

[8] D. Branford, Part. Nucl. 6, 127 (1974).

[9] E. M. Diener, J. F. Amann, and P. Paul, Phys. Rev. C 7, 695 (1973).

[10] D. Brajnik, D. Jamnik, G. Kernel, U. Miklavzic, and A. Stanovnik, Phys. Rev. C 9, 1901 (1974).

[11] See, e.g., J. S. O'Connell, in Proceedings of the International Conference on Photonuclear Reactions and Applications, Asilomar, 1973, edited by B. L. Berman (Lawrence Livermore Laboratory, Univ. of California, 1973), p. 71.

[12] N. T. Porile, in Nuclear Chemistry, edited by L. Yaffe (Academic, New York, 1968), p. 110.

[13] J. D. Sherman, D. L. Hendrie, and M. S. Zisman, Phys. Rev. C 13, 20 (1976).

[14] G. R. Satchler, Nucl. Phys. 55, 1 (1964).

[15] Received from P. D. Kunz, Univ. of Colorado (unpublished).

[16] T. Kishimoto (private communication).

[17] L. Zamick (private communication).

[18] R. L. Kozub, Phys. Rev. 172, 1078 (1968).

[19] J. B. Marion and F. C. Young, Nuclear Reaction Analysis: Graphs and Tables (North-Holland, Amsterdam, 1968), p. 86.

[20] A. Moalem, W. Benenson, G. M. Crawley, and T. L. Khoo, Phys. Lett. 61B, 167 (1976).